Presented at 2019 RVP-AI Conference

Power Swing Detection and Monitoring using Digital Fault Recorders

Adeyemi Charles Adewole
ERLPhase Power Technologies
Winnipeg, Canada
cadewole@erlphase.com

Ponram Karrupiah
ERLPhase Power Technologies
Winnipeg, Canada
pkarrupiah@erlphase.com

Nuwan Perera
ERLPhase Power Technologies
Winnipeg, Canada
nperera@erlphase.com

Hector Ponce
ERLPhase Power Technologies
Winnipeg, Canada
hponce@erlphase.com

René Midence
ERLPhase Power Technologies
Winnipeg, Canada
rmidence@erlphase.com

***Abstract*—Power swings can cause unnecessary protective relay operations in power systems, resulting in cascading blackouts. This paper investigates the detection of power swings on transmission lines using Digital Fault Recorders (DFRs). Various power swing conditions were generated using electromagnetic transient simulations carried out in PSCAD/EMTDCTM. The disturbance records generated were played back onto a DFR, and a power swing detection and monitoring algorithm implemented in the DFR was used in detecting the presence of power swing conditions. Results obtained were promising and demonstrated how DFRs can be deployed as a monitoring system suitable for triggering the capture of abnormal events such as power swing events.**

***Keywords*—DFRs, Distance relays, disturbance recording, power swing, protective relaying.**

I. Background

Power swings are oscillations in real and reactive power flows on a transmission line resulting from faults, load variation, and switching actions. Power swings on a transmission line can cause the load impedance to encroach into the operating characteristic of a distance protective relay, thereby resulting in unnecessary operation of the distance protection and the incorrect tripping of the transmission lines in the system. Thus, leading to blackouts.

Increased power transfer has been known to cause load impedances to enter the operating characteristic of zone 3 backup distance protection relays and the consequent unnecessary operation of zone 3 distance protection element [1]. Such load responsive protective relay elements are required by the North American Electric Reliability Corporation (NERC) not to trip for stable power swings during unfaulted conditions [1]. Most distance protective relays have a power swing blocking functionality which is used to differentiate between faults and power swing conditions, and restrain the relay from operating for power swing conditions.

The impact of power swing and the nuisance tripping of distance protective relaying can be very devasting to power system stability. Thus, system operators need tools that can be used to help them understand, predict, and identify the onset of power swing conditions timely before they occur. This paper proposes the use of a DFR as a disturbance monitoring system that can be applied for identifying power swing conditions in power systems. The remainder of this paper is organized as follows: Section II introduces the power swing phenomenon and some detection methods available in the literature, while Section III describes the proposed algorithm. Section IV presents the modelling, proof-of-concept testbed, and some of the results obtained. Section V summarizes the contribution of the paper.

II. Power Swing Detection

The real power (P) transmitted in a simple lossless transmission line with sources at both ends (Fig. 1) is given by:

$$P = \frac{|E_S||E_R|}{X} \sin(\delta) \quad (8)$$

where E_S and E_R are the sending and receiving end voltages, δ is the angle between E_S and E_R, and X is the total reactance between E_S and E_R.

A power angle curve can be used to show the relationship between P and δ as shown in Fig. 2. From Fig. 2, it can be seen that the transmitted power increases as δ increases. The maximum power is obtained when δ equals 90°, and the power transfer decreases as δ increases. The steady-state operating condition is at (P_0, δ_0) as shown in Fig. 2.

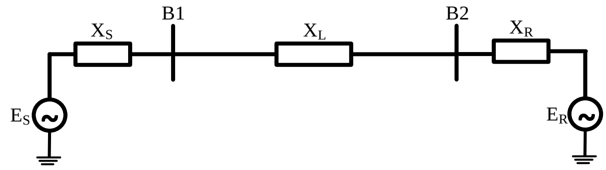

Fig. 1. Equivalent two-source system.

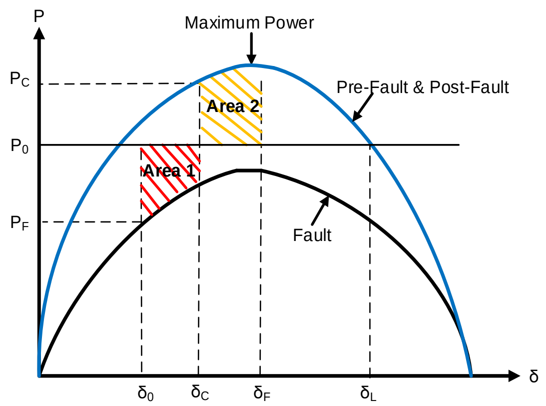

Fig. 2. System stable clearing time.

At steady-state, the mechanical input power is converted to its equivalent electrical output power with an angle δ between E_S and E_R, and a constant system frequency. In the event of a fault, the electrical power will reduce to P_F and the generator will accelerate because its input mechanical power cannot be instantly decreased. Consequently, the post-fault angle is at δ_C and the electrical power output is greater than the mechanical input power. Thus, causing the generator to decelerate. The inertia of the generator rotor causes the angle to increase to angle δ_F. For a stable system, the energy lost in Area 2 is equal to the energy gained in Area 1. This is known as the Equal Area Criterion (EAC). For an unstable condition, Area 2 is smaller than Area 1 as shown in Fig. 3. Thus, the angle will increase to δ_L or beyond. When this occurs, one of the generators in the system will rotate at a different speed. Thereby causing an unstable power swing or out-of-step condition.

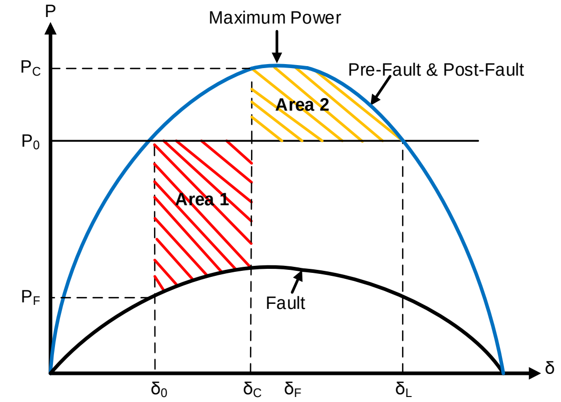

Fig. 3. System unstable clearing time (slow time).

Power swing detection can be generally categorized into two. These are i) conventional methods, and non-conventional methods.

The principle behind conventional power swing detection is based on the fact that the apparent impedance travels with a relatively slow pace during power swing conditions and travels faster during faults. Zones of interests can be formed using blinders, quadrilaterals, or Mho characteristics as shown in Figs. 4-6.

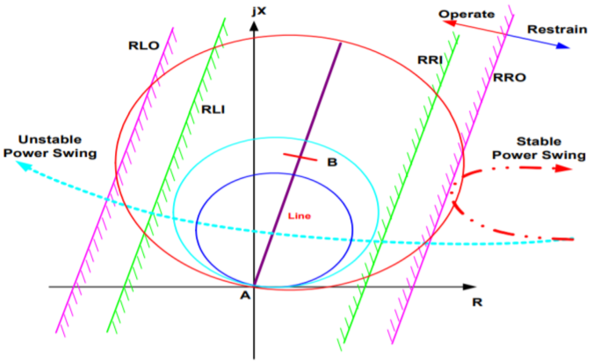

Fig. 4. Double blinder impedance-based PSD characteristic [1].

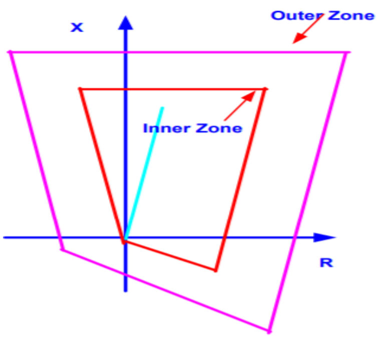

Fig. 5. Concentric quadrilateral PSD characteristic [1].

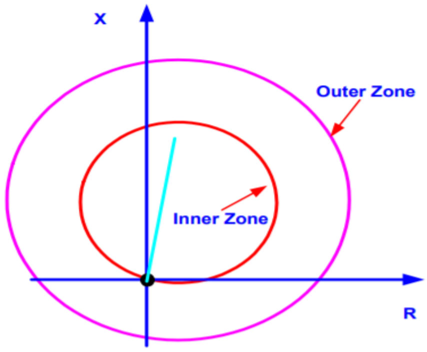

Fig. 6. Concentric Mho PSD technique [1].

Non-conventional power swing detection methods include the rate of change of resistance [2]-[4], swing center voltage and its rate of change [5], and synchrophasor-based methods [6].

III. Disturbance Recording

Disturbance records are essential in the identification of the cause of a fault or abnormal condition, the severity of these conditions, and the evaluation of the performance of the associated protective or control devices implemented in the power system. These records also show the dynamic response of the system during power swings, system stability conditions, power quality conditions, and for post-mortem analysis of wide area disturbances.

Four types of disturbances can occur in power systems [7]. These are: i) steady-state disturbances, ii) transient disturbances, iii) short-term disturbances, and iv) long-term disturbances. Steady-state disturbances occur during normal system operating condition. The system operation is not at risk during such disturbances, but power quality issues such as harmonics and sub-harmonics could ensue. Transient disturbances are brief faults with a short duration of 8-16 cycles [7]. Short-term disturbances include events with time delayed clearance and reclosing events. They are usually longer than transient disturbances and have a duration of 20-60 cycles. Long-term disturbances affect the stability of the system and are associated with rotor angle stability, frequency stability, and voltage stability respectively. Long term disturbances have a longer duration and could last for days.

The capture of disturbance recordings can be initiated using triggers. These triggers can be measured or calculated analogue channels of magnitude (voltage, current, frequency, real power, reactive power, and apparent impedance), rate of change (voltage, current, frequency, real power, reactive power, and apparent impedance), harmonic, voltage sags and swells. Also, external inputs, binary signals (breakers, protection trip, communication-assisted key), or programmable logic can be used.

Figs. 7-8 shows the two types of triggering possible [7]. For edge triggering, the recording is initiated at the rising edge of the trigger (Fig. 7), and the recording is captured for a pre-determined length of time. The length of the recording depends on the amount of pre-fault data, the length of the fault, and the amount of post-fault data. Duration triggering keeps recording for as long as the trigger is asserted as shown in Fig. 8.

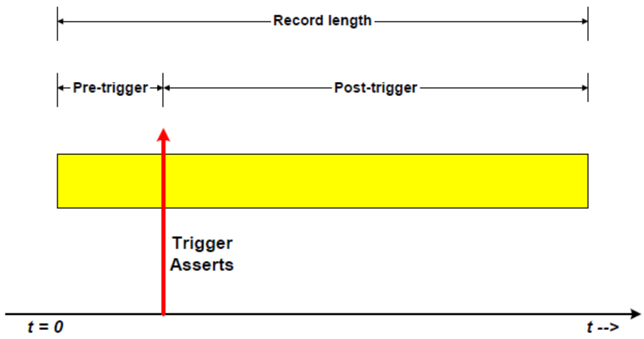

Fig. 7. Disturbance record length using edge triggering [7].

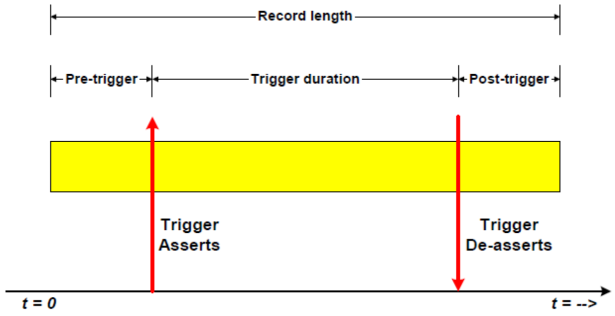

Fig. 8. Disturbance record length using duration triggering [7].

Fig. 9 demonstrates the basic operation of the power swing detection algorithm. The variation of the positive sequence impedance calculated from three phase voltage and current measuements are monitored to identify power swing conditions using dual (outer and inner) Mho impedance characteristics. The time taken to cross the outer and inner Mho characteristic is measured. If the time taken (T2-T1 shown in Fig. 10) exceeds the threshold time (user-defined time), the event is declared as a power swing condition. It should be noted that any operating conditions in which the trajectory stays within the Mho impedance characteristic for more than the user-defined duration will be declared as an active power swing condtion. This algorithm has been adapted from the power swing algorithm available in [8]. The power swing detector algoritum can also be supervised using negative sequence and zero sequence currents, respectively. This provides an extra security to the power swing detector logic. Fig. 10 shows an example logic created with a power swing detector monitored using the negative sequence and zero sequence currents.

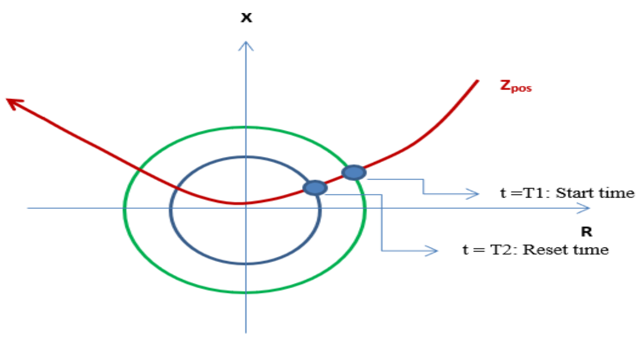

Fig. 9. Power swing detection principle.

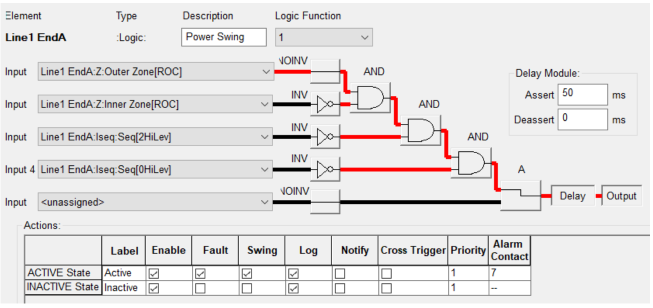

Fig. 10. Power swing detection algorithm.

IV. Implementation and Test Cases

This section presents the implementation procedure and the test cases considered.

A. Test System Modelling

Fig. 11 shows the IEEE EMTP reference model for transmission line protective relaying testing [9] which was modelled in PSCAD-EMTDC^{TM} and used in generating the disturbances record required for testing the power swing detection algorithm.

The reference model is a 230 kV network with two sources at buses B1 and B3 modelled with an impedance and a generator at B4 connected via transformer TR1. A third line tapped off at the middle of the parallel transmission line has a switch which is left open throughout the simulations carried out in this paper. Further details on the system parameters can be found in [9].

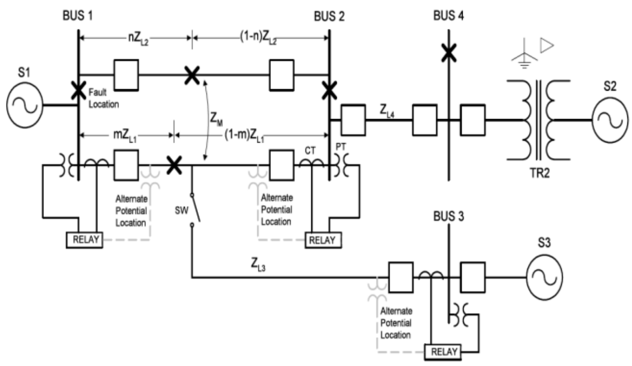

Fig. 11. IEEE EMTP reference model.

B. Playback Implementation

The power swing event captured in PSCAD are saved as COMTRADE header, configuration, and data (.HDR, .CFG and .DAT) files, respectively. The .HDR file is a human readable ASCII text file, while the .CFG file provides the translation guideline for the .DAT file, and it contains all the necessary details regarding the disturbance record. Some of these information are the station name and identification, the total number of analogue and digital channels, the data for each of the analogue and digital channels, frequency, sample rate and number of samples, date and time of the first data point and the trigger point, and the data file format (ASCII or binary).

Similarly, the .DAT file contains the actual instantaneous sampled data from the analogue and digital channels, respectively. The analogue channels were used in this paper for recording the three phase currents and voltages, while the digital channel of the disturbance was used for recording the fault inception bits. The data can be stored in the ASCII or binary format. The voltage and current signals in the COMTRADE files transferred to the DFR using a playback testset as shown in Fig. 12.

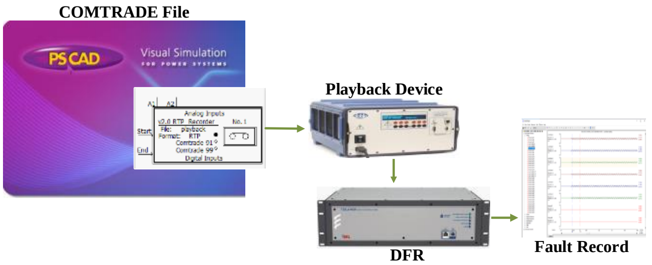

Fig. 12. Playback implementation setup.

C. Case Studies and Results

In order to simulate a power swing, a three-phase fault was applied at bus B1and was cleared after 200 ms. Figs. 13. (a) and (b) show the three phase voltages measured by a VT connected to B2 and the R-X plot showing the protection zones (zones 1-3), inner and outer concentric circle characteristics, and the trajectory of the calculated impedance.

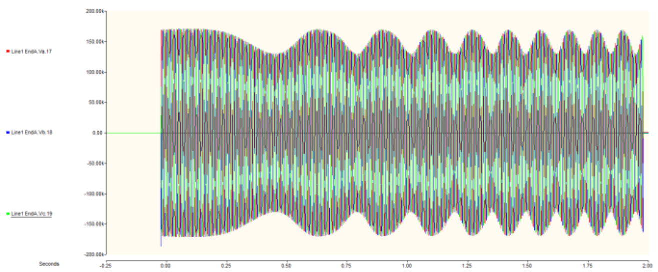

(a)

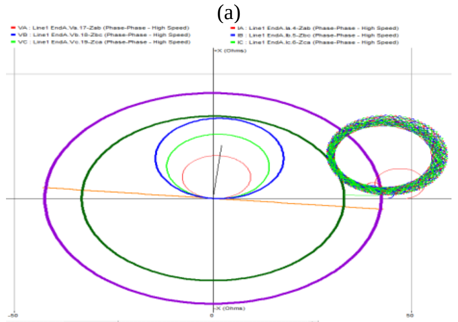

(b)

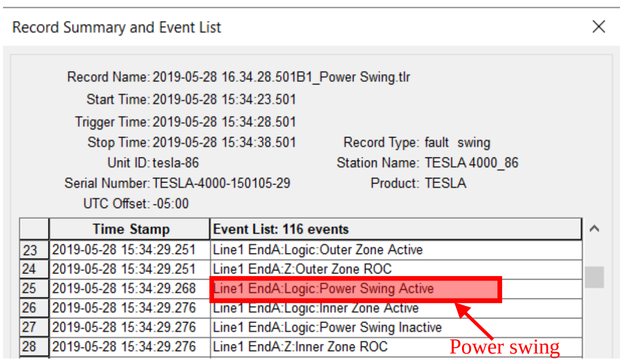

	Time Stamp	Event List: 116 events
23	2019-05-28 15:34:29.251	Line1 EndA:Logic:Outer Zone Active
24	2019-05-28 15:34:29.251	Line1 EndA:Z:Outer Zone ROC
25	2019-05-28 15:34:29.268	Line1 EndA:Logic:Power Swing Active
26	2019-05-28 15:34:29.276	Line1 EndA:Logic:Inner Zone Active
27	2019-05-28 15:34:29.276	Line1 EndA:Logic:Power Swing Inactive
28	2019-05-28 15:34:29.276	Line1 EndA:Z:Inner Zone ROC

(c)

Fig. 13. Power swing condition (a) Three-phase voltages, (b) calculated impedance (c) sequence of events list.

The proposed algorithm correctly detected the multiple power swings that occurred in this case as shown in the sequence of events record in Fig. 13(c). Fig. 14 shows the result for a power swing condition that ensued after a three phase fault at B1 with an A-g fault applied during the power swing. The DFR was able to accurately detect both the power swing and the fault conditions as they occurred.

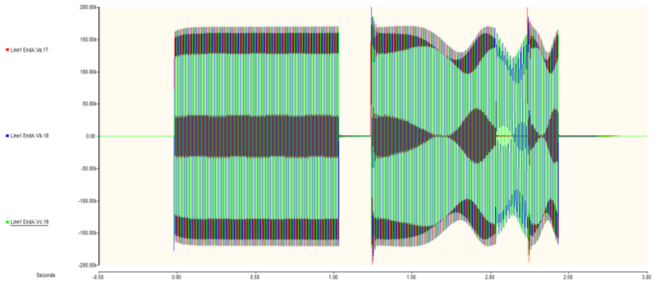

(a)

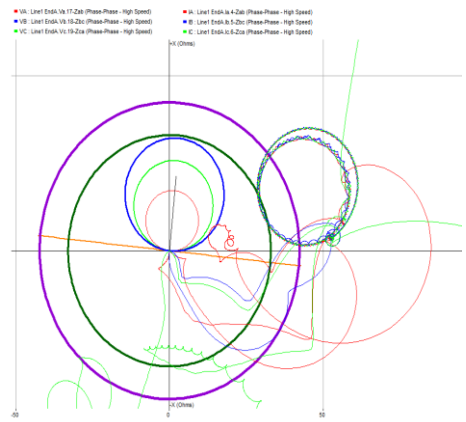

(b)

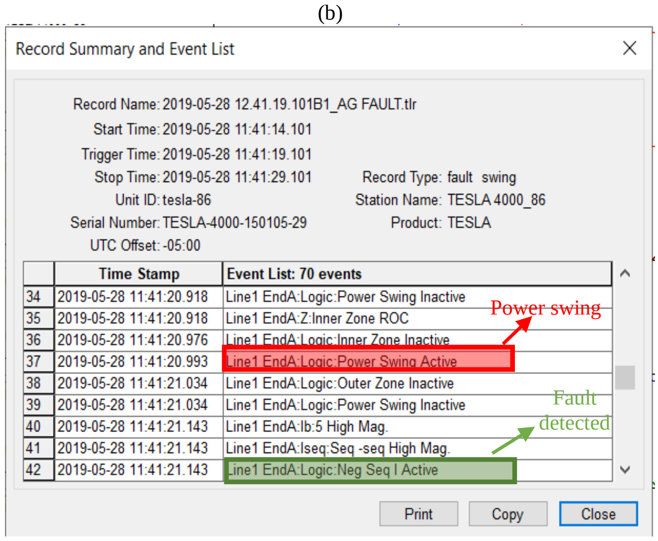

	Time Stamp	Event List: 70 events
34	2019-05-28 11:41:20.918	Line1 EndA:Logic:Power Swing Inactive
35	2019-05-28 11:41:20.918	Line1 EndA:Z:Inner Zone ROC
36	2019-05-28 11:41:20.976	Line1 EndA:Logic:Inner Zone Inactive
37	2019-05-28 11:41:20.993	Line1 EndA:Logic:Power Swing Active
38	2019-05-28 11:41:21.034	Line1 EndA:Logic:Outer Zone Inactive
39	2019-05-28 11:41:21.034	Line1 EndA:Logic:Power Swing Inactive
40	2019-05-28 11:41:21.143	Line1 EndA:Ib:5 High Mag.
41	2019-05-28 11:41:21.143	Line1 EndA:Iseq:Seq -seq High Mag.
42	2019-05-28 11:41:21.143	Line1 EndA:Logic:Neg Seq I Active

(c)

Fig. 14. Power swing condition with A-g bus fault during swing (a) Three-phase voltages, (b) calculated impedance (c) sequence of events..

The proposed algorithm was able to correctly detect the presence of power swings for the scenario shown in Fig. 15, and correctly deasserted for the three phase fault condition that ensued afterwards. Similar results were obtained for a BC-g fault with a fault resistance of 20 Ω (Fig. 16) and an ABC fault at 50% of Line 1 (Fig. 17).

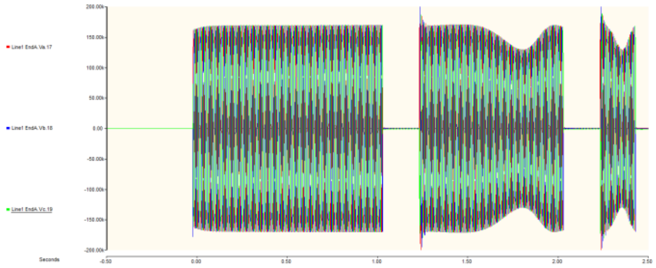

(a)

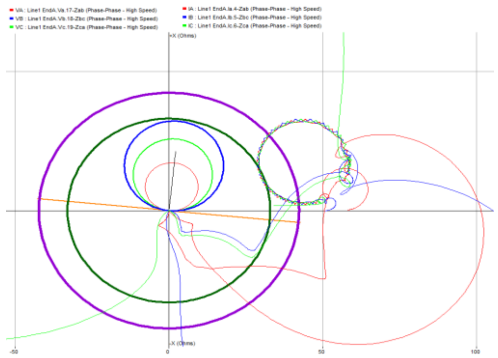

(b)

Fig. 15. Power swing condition with ABC bus fault during swing (a) Three-phase voltages, (b) calculated impedance.

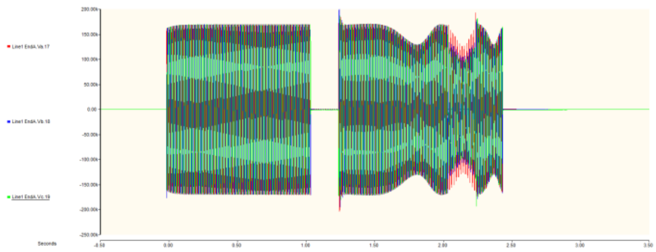

(a)

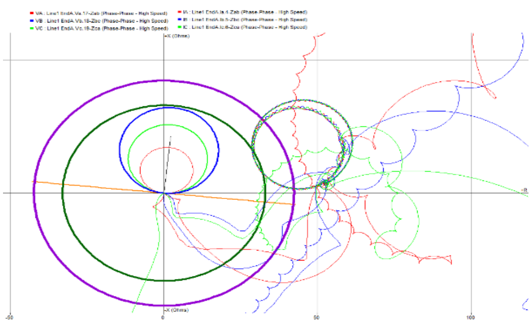

(b)

Fig. 16. Power swing condition with a 20 Ω BC-g bus fault during swing (a) Three-phase voltages, (b) calculated impedance.

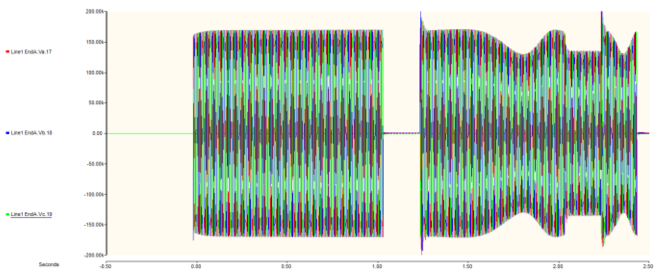

(a)

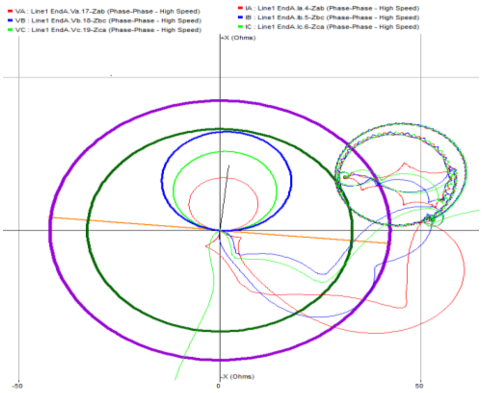

(b)

Fig. 17. Power swing condition for ABC fault at 50% of Line 1 (a) Three-phase voltages, (b) calculated impedance.

V. Conclusion

This paper explored the use of a DFR for monitoring and detecting power swings using an algorithm based on the rate of change of impedance. Several scenarios were considered for swing-only condition, fault during power swing, various fault locations, fault types, and fault resistances. Results showed that the DFR was able to detect faults, power swings, and fault conditions that occurred during power swings. The robustness of the proposed algorithm was demonstrated for various swing frequencies. The results obtained demonstrated the possibility of using DFRs for power system monitoring and the detection of abnormal condition.

References

[1] Power Swing and Out-Of-Step Considerations on Transmission Lines, IEEE PSRC WG D6, Power System Relaying Committee (PSRC) of the IEEE Power Engineering Society, 2005. [Online]. Available: www.pes-psrc.org

[2] J. Holbach, "New Out-of-Step Blocking Algorithm for Detecting Fast Power Swing Frequencies," Proceedings of the 30th Annual Western *Protective Relay Conference*, Spokane, WA, October 21–23, 2003.

[3] C. W. Taylor, "A New Out-of-Step Relay With Rate of Change of Apparent Resistance Augmentation," IEEE Transactions on Power Apparatus and Systems, Vol. 102, No. 3, pp. 631–639, March 1983.

[4] J. M. Haner, T. D. Laughlin, and C. W. Taylor, "Experience With the Rdot Out-of-Step Relay," IEEE Transactions on Power Delivery, Vol. 1, No. 3, pp. 35–39, April 1986.

[5] G. Benmouyal, D. Hou, and D. Tziouvaras, "Zero-setting power swing blocking protection," proceedings of the 31st Annual Western Protective Relay Conference, Spokane, WA, October 2004.

[6] E. O. Schweitzer III, G. Benmouyal, and A. Guzmán, "Synchronized Phasor Measurement in Protective Relays for Protection, Control, and Analysis of Electrical Power Systems," Proceedings of the *29th Annual* Western

[7] Considerations for Use of Disturbance Recorders, Report to the System Protection Subcommittee of the Power System Relaying Committee (PSRC) of the IEEE Power Engineering Society, 2006. [Online]. Available: www.pes-psrc.org

[8] L-PRO 4000 Transmission Line Protection Relay User Manual Version 2.5 Rev 1.

Power System Relaying Committee, "EMTP reference models for transmission line relay testing," Final Technical Report, 2005. [Online]. Available: www.pes-psrc.org